Cardiomyocytes derived from human embryonic and induced pluripotent stem cells: comparative ultrastructure

Mihaela Gherghiceanu [a, #], **Lili Barad** [b, c, d, #], **Atara Novak** [b, c, d], **Irina Reiter** [b, c, d],
Joseph Itskovitz-Eldor [b, d, e], **Ofer Binah** [b, c, d, *], **L.M. Popescu** [a, f, *]

[a] *'Victor Babeş' National Institute of Pathology, Bucharest, Romania*
[b] *The Sohnis Family Stem Cells Center, Haifa, Israel*
[c] *The Rappaport Institute, Haifa, Israel*
[d] *Rappaport Faculty of Medicine, Technion, Haifa, Israel*
[e] *Department of Obstetrics and Gynecology, Rambam Health Care Campus, Haifa, Israel*
[f] *Department of Cellular and Molecular Medicine, 'Carol Davila' University of Medicine and Pharmacy, Bucharest, Romania*

Abstract

Induced pluripotent stem cells (iPSC) are generated from fully differentiated somatic cells that were reprogrammed into a pluripotent state. Human iPSC which can be obtained from various types of somatic cells such as fibroblasts or keratinocytes can differentiate into cardiomyocytes (iPSC-CM), which exhibit cardiac-like transmembrane action potentials, intracellular Ca^{2+} transients and contractions. While major features of the excitation-contraction coupling of iPSC-CM have been well-described, very little is known on the ultrastructure of these cardiomyocytes. The ultrastructural features of 31-day-old (post-plating) iPSC-CM generated from human hair follicle keratinocytes (HFKT-iPSC-CM) were analysed by electron microscopy, and compared with those of human embryonic stem-cell-derived cardiomyocytes (hESC-CM). The comparison showed that cardiomyocytes from the two sources share similar proprieties. Specifically, HFKT-iPSC-CM and hESC-CM, displayed ultrastructural features of early and immature phenotype: myofibrils with sarcomeric pattern, large glycogen deposits, lipid droplets, long and slender mitochondria, free ribosomes, rough endoplasmic reticulum, sarcoplasmic reticulum and caveolae. Noteworthy, the SR is less developed in HFKT-iPSC-CM. We also found in both cell types: (1) 'Ca^{2+}-release units', which connect the peripheral sarcoplasmic reticulum with plasmalemma; and (2) intercellular junctions, which mimic intercalated disks (desmosomes and fascia adherens). In conclusion, iPSC and hESC differentiate into cardiomyocytes of comparable ultrastructure, thus supporting the notion that iPSC offer a viable option for an autologous cell source for cardiac regenerative therapy.

Keywords: induced pluripotent stem cells ● human embryonic stem cells ● cardiomyocytes ● Ca^{2+}-release units ● sarcoplasmic reticulum ● action potentials ● caveolae

Introduction

Induced pluripotent stem cells, which represent an ideal cell source for future cell therapy and regenerative medicine [1, 2], can differentiate into fully functional cardiomyocytes (CM) exhibiting cardiac-like transmembrane action potentials, intracellular Ca^{2+} transients and contractions, as well as responsiveness to autonomic agonists and antagonists [3, 4]. While most iPSC lines described so far were derived from dermal fibroblasts or other cell sources which require harvesting by surgical intervention, we

---

[#]Both the authors contributed equally to this work.
*Correspondence to: Ofer BINAH,
Department of Physiology, Ruth & Bruce Rappaport Faculty of Medicine,
P.O. Box 9649, Haifa 31096, Israel.
Tel.: +972-48295262
Fax: +972-48513919
E-mail: binah@tx.technion.ac.il

L.M. POPESCU,
Department of Cellular and Molecular Medicine,
'Carol Davila' University of Medicine and Pharmacy,
P.O. Box 35-29, Bucharest 35, Romania.
Tel.: +40-744-535298
Fax: +40-21-3124885
E-mail: lpopescu@jcmm.org

recently reported the successful generation of iPSC derived from HFKT [4]. The HFKT-iPSC-derived spontaneously beating cardiomyocytes (HFKT-iPSC-CM) displayed well-coordinated intracellular Ca^{2+} transients and contractions which were readily responsive to β-adrenergic stimulation with isoproterenol.

Although major aspects of the excitation–contraction coupling of iPSC-CM have been well-described, almost nothing is known on the ultrastructural characteristics of these cardiomyocytes. In this regards, Fujiwara et al. [5] suggested that iPSC-CM generated from human adult fibroblasts have some ultrastructural features of cardiomyocytes. The aim of this study was to investigate in details the ultrastructural characteristics of cardiomyocytes derived from iPSC. Specifically, 31-day-old (post-plating) HFKT-iPSC-CM, were analysed, and compared to hESC-CM.

Here we report that HFKT-iPSC-CM and hESC-CM have similar ultrastructure, thus supporting the view that iPSC provide a viable autologous cell source for cardiac regenerative therapy.

Materials and methods

Generation of hESC-CM and HFKT-iPSC-CM

iPSC were generated from human hair follicle keratinocytes as detailed in our recent publication [4]. hESC from clone H9.2 were grown on mouse embryonic fibroblast feeder as previously described [6]. hESC and iPSC were spontaneously differentiated towards embryoid bodies (EBs) and cardiomyocytes as previously described [3, 6].

Microelectrode array (MEA) recordings

Extracellular electrograms were recorded from spontaneously contracting EBs, using the MEA set-up (Multi Channels Systems, Reutlingen, Germany) as previously described [4, 7, 8].

Whole-cell current clamp recordings

For the current clamp studies spontaneously beating small cell clusters or isolated cells produced after dissociation of the HFKT-iPSC-CM were studied following plating on top of gelatin or fibronectin-coated glass cover slips. The patch pipette solution contained (mM): 120 KCl, 1 MgCl$_2$, 3 Mg-ATP, 10 HEPES, 10 EGTA (pH 7.3). The bath solution contained (mM): 140 NaCl, 5.4 KCl, 1.8 CaCl$_2$, 1 MgCl$_2$, 10 HEPES, 10 glucose (pH 7.4) (all materials from Sigma-Aldrich, St. Louis, MO, USA). Action potentials were recorded using the current clamp mode. Axopatch 200B, Digidata 1322 and pClamp10 (Molecular Devices, Sunnyvale, CA, USA) were used for data amplification, acquisition and analysis.

Transmission electron microscopy

Transmission electron microscopy (TEM) was performed on 31-day-old (post-plating) EBs derived from HFKT-iPSC and hESC fixed with 2.5% glutaraldehyde in 0.1M cacodylate buffer [pH 7.4, room temperature (RT)]. The samples were post-fixed for 1 hr in buffered 1% OsO$_4$ with 1.5% K4Fe(CN)6 (potassium ferrocyanide-reduced osmium) at RT. Fixed EBs were embedded in 1% agar, dehydrated in graded ethanol series and further processed for epoxy resin (Agar100) embedded at 60°C for 48 hrs [9, 10]. One-micrometre-thick sections (semi-thin sections) were stained with 1% toluidine blue (blue sections) and examined by light microscopy. The ultra-thin sections were cut with a diamond knife at 60 nm thicknesses using an RMC ultramicrotome (Boeckeler Instruments Inc., Tucson, AZ, USA) and double stained with 1% uranyl acetate and Reynolds lead citrate. Ultrastructural examination was performed with a Morgagni 286 transmission electron microscope (FEI Company, Eindhoven, The Netherlands) at 60 kV. Digital electron micrographs were recorded with a MegaView III CCD and iTEM-SIS software (Olympus, Soft Imaging System GmbH, Münster, Germany) was used for morphometry. The lengths and widths of cardiomyocytes were considered as the largest and smallest dimension of cross-sectioned cells, and were expressed in micrometre. Nucleo-cytoplasmic ratio (N/C) was calculated as the ratio between the measured cross-sectional areas (μm^2) of the nucleus and the cytoplasm measured with iTEM software. In each group of EBs, we randomly chose cells to measure the nucleus/cell area ratio, cell dimensions and Z bands. Twenty-eight cells with visible nucleus were measured on 25 randomly-selected electron micrographs at lower magnification for each sample (HFKT-iPSC-CM and hESC-CM). The images were made on three EBs containing HFKT-iPSC-CM and three EBs containing hESC-CM. The areas of nucleus and cell body, and the maximum length and width were measured. Nucleo-cytoplasmic ratio was calculated as the ratio between the measured cross-sectional areas of the nucleus and the cytoplasm. The Z-like structures were counted in 28 cells. The sarcomeres dimension was measured on 10 cells having at least two sarcomeres.

Semi-quantitative assessment was made on 25 electron micrographs at lower magnification (5400×) for each sample. To evaluate the amount of organelles (mitochondria, endoplasmic reticulum, lipid droplets, glycogen, sarcomeres), a scoring system was employed in cardiomyocytes using the ultrastructure of embryonic stem cells as a reference (0: few isolated organelles; 1: small groups of 3–5 organelles or 25% of cells; 2: groups of 5–10 organelles or 50%; 3: numerous groups of organelles or >50%).

Statistical analysis

The morphometric parameters of width and length of cardiomyocytes were compared by means of the Student's t-test for unpaired observations.

Results

HFKT-iPSC-CM physiology

The functionality of the iPSC-CM is illustrated by robust extracellular electrograms recorded by the MEA data acquisition system (Fig. 1A). In addition, the functionality of these cells is also demonstrated by representative recordings of spontaneous generated action potentials with prominent pacemaker potential (Fig. 1B). Similar results were obtained in eight preparations and were previously described [4].
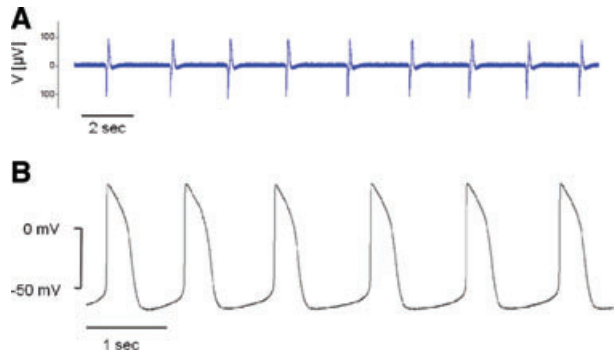
Fig. 1 Electrophysiological features of cardiomyocytes derived from iPSC generated from human plucked hair follicle keratinocytes (HFKT-iPSC-CM; clone KTN3). (**A**) Extracellular electrograms recorded by means of MEA data acquisition system from a spontaneously contracting embryoid body (EB). (**B**) Representative action potential recordings from a spontaneously contracting EB (clone KTN3), demonstrating the pacemaker activity of the HFKT-iPSC-CM.

The overall ultrastructural features of EBs

Light microscopy inspection of semi-thin sections from resin-embedded samples revealed EBs as spherical dense cellular colonies in both HFKT-iPSC-CM (Fig. 2A) and hESC-CM (Fig. 2B).

As shown in Figure 3 (blue sections, insets), the cells in the periphery of the EB were elongated with a rod-shaped morphology, and often a clear cross-striations pattern of myofibrils was visible in the cytoplasm (Fig. 3). In contrast, the centrally-located cardiomyocytes were densely packed, round-shaped, with no visible striations, but with numerous lipid vacuoles and glycogen content (Fig. 4, blue sections, insets). Electron microscopy showed that all EBs contain similar cells with ultrastructural features of cardiomyocytes (Figs 3 and 4) surrounded by a monolayer of epithelial cells. The HFKT-iPSC-CM (Fig. 3A) and hESC-CM (Fig. 3B) from the EBs periphery were more elongated than cells in the centre which had an irregular shape with a round oval cellular body and short intermeshed cellular processes (Fig. 4A and B). Small cellular spaces containing collagen fibrils and cellular debris were present in between differentiated cardiomyocytes in the centre of EBs. The nuclei of the cardiomyocytes were more oval in the periphery (Fig. 3) than in the centre (Fig. 4) of the EBs where they showed a slightly irregular contour.

Comparative structural analysis of HFKT-iPSC-CM and hESC-CM

Our findings show that HFKT-iPSC-CM and hESC-CM differ quantitatively in several structural parameters. As seen in Figure 5, the lengths of the cardiomyocytes were distributed differently
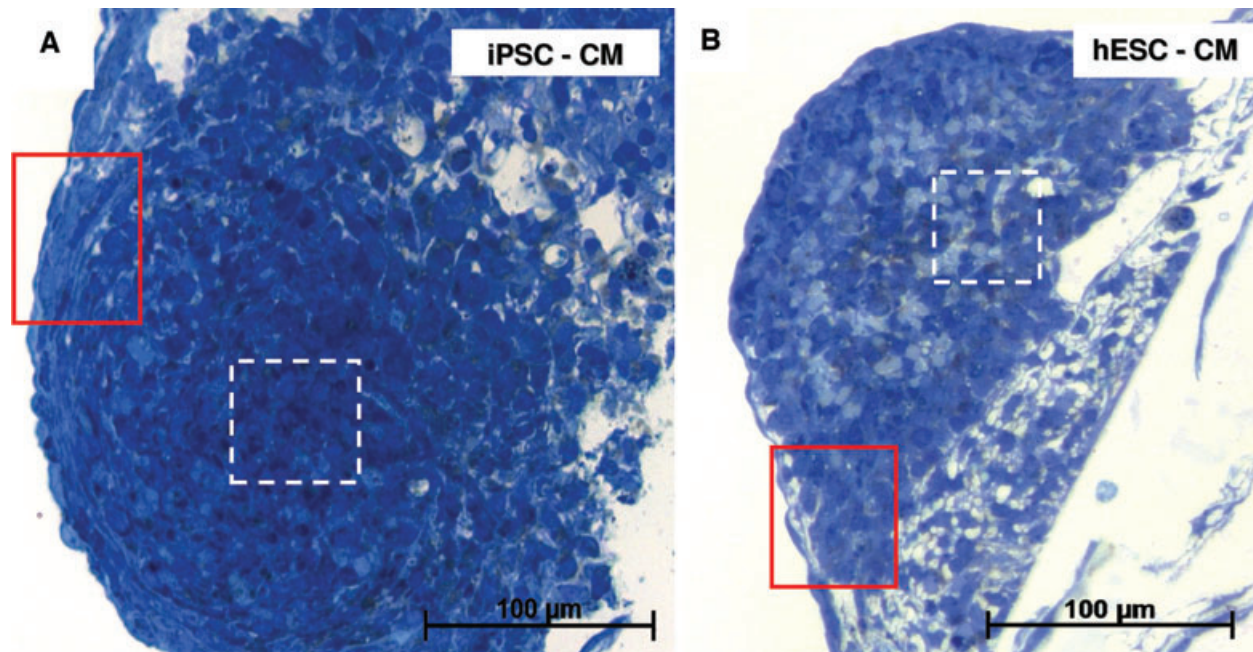

Fig. 2 Light microscopy of semi-thin sections. Toluidine blue staining of resin-embedded embryoid bodies of HFKT-iPSC (**A**) and hESC (**B**). The red squared marked areas in the periphery of EBs in (**A**) and (**B**) have the corresponding light and electron microscopy in Figure 3. Light and electron microscopy of areas marked with white dashed lines in (**A**) and (**B**) are detailed in Figure 4.
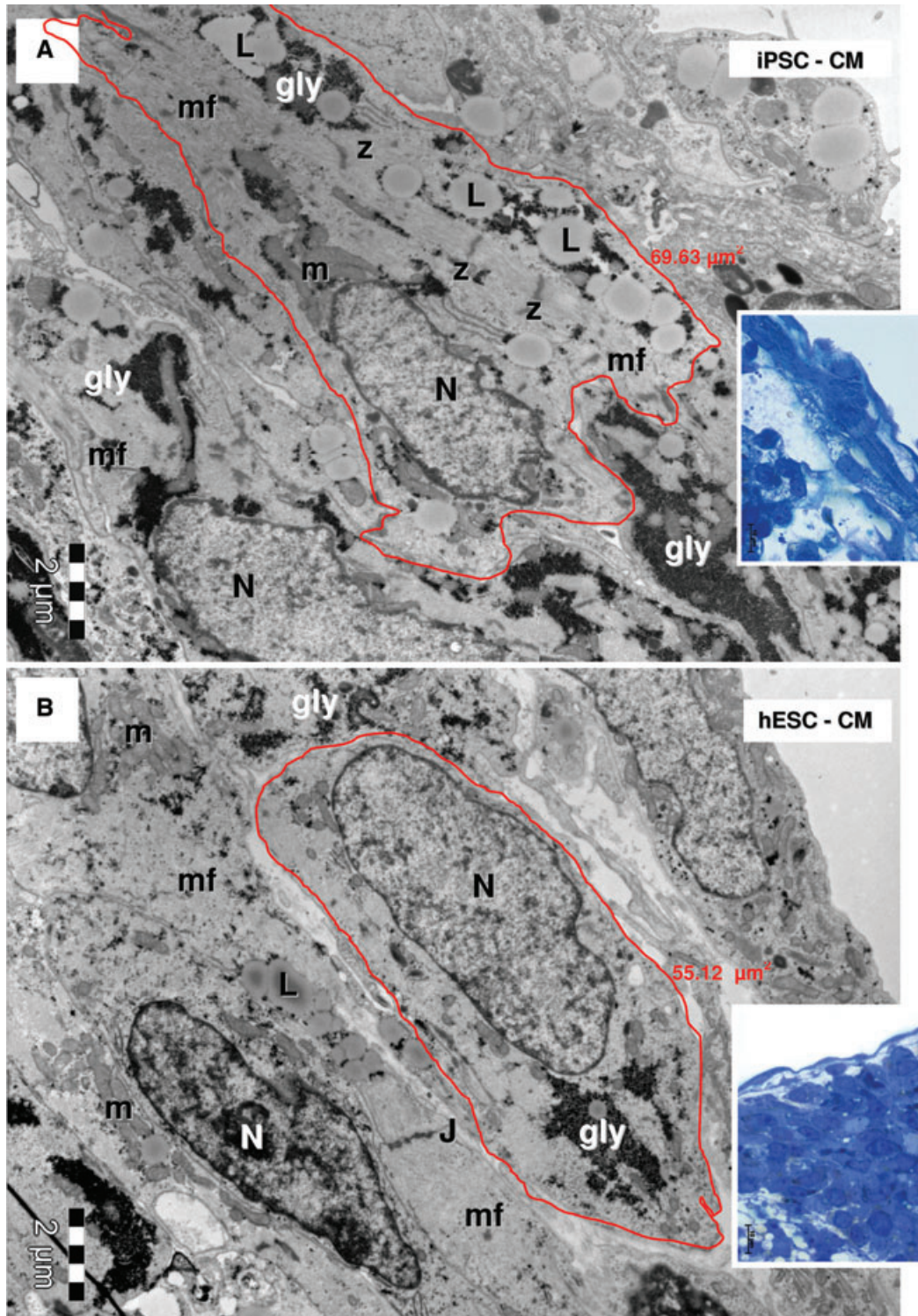
Fig. 3 Electron micrographs of the EBs periphery (red marked areas in Fig. 1A and B, higher magnification of blue sections in the corresponding insets) show ellipsoid cardiomyocytes derived from HFK-iPSC (**A**) and hESC (**B**). Myofilaments (mf) organized in distinct sarcomeric structures delineated by Z-bands. Lipid droplets (L), glycogen masses (gly) and clusters of mitochondria (m) are visible in cytoplasm of cardiomyocytes. Small junctions (J) connect the cardiomyocytes. N: nucleus. The measured areas of red outlined cardiomyocytes are 69.63 μm^2 for HFK-iPSC-CM (**A**) and 55.12 μm^2 for hESC-CM (**B**).
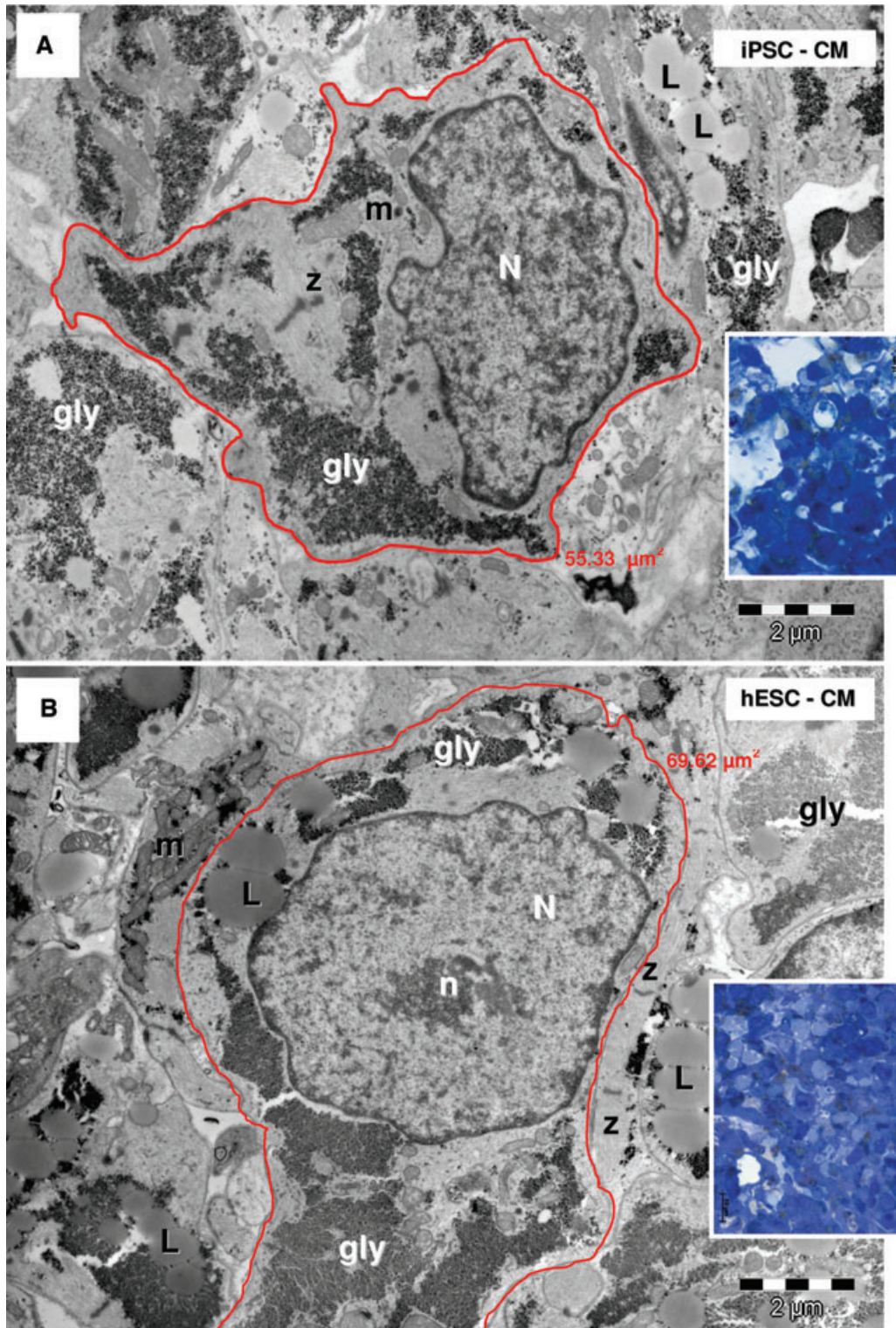
Fig. 4 Electron micrographs of the EBs centre (white marked areas in Fig. 2A and B) show cardiomyocytes with irregular contour derived from HFK-iPSC (**A**) and hESC (**B**). Insets show corresponding blue sections. Cardiomyocytes have myofibrils (mf), Z-bands, lipid droplets (L), glycogen (gly), mitochondria (m). N: nucleus; n: nucleolus. The measured areas of red outlined cardiomyocytes are 55.33 μm^2 for HFK-iPSC-CM (**A**) and 69.62 μm^2 for hESC-CM (**B**).
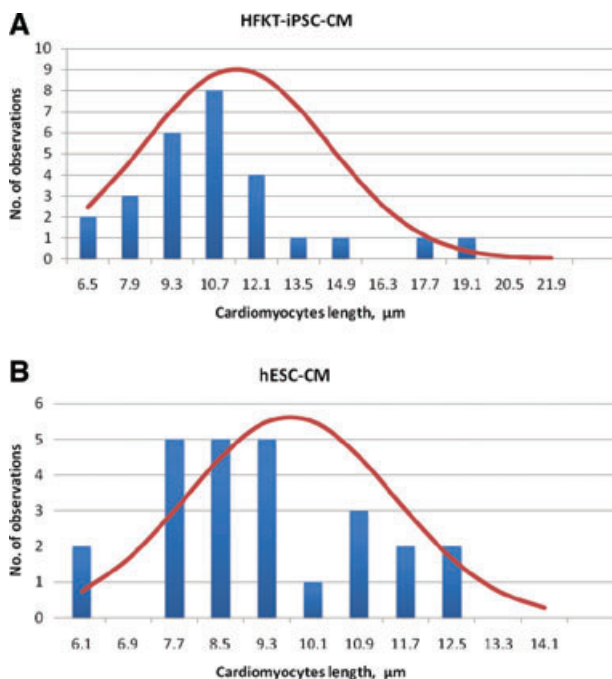
Fig. 5 Histograms for measured lengths of HFK-iPSC-CM (**A**) and hESC-CM (**B**). The red line represents the ideal situation. In each group, 28 cardiomyocytes were analysed. The analysis included three EBs from each group.

within the two groups. Accordingly, as seen in Table 1, cell length was larger in HFKT-iPSC-CM (11.93 $\pm$ 3.99) than in hESC-CM (9.68 + 3.06, $P < 0.05$). In addition, cell area and cytoplasm area were also larger ($P < 0.05$) in HFKT-iPSC-CM than hESC-CM. The differences in other parameters were not statistically different between the groups.

Comparative ultrastructural analysis of HFKT-iPSC-CM and hESC-CM

Both HFKT-iPSC-CM (Figs 3A and 4A) and hESC-CM (Figs 3B and 4B) showed ultrastructural features of early (centre of EB; Fig. 4) and immature cardiac phenotype (periphery of EB; Fig. 3) containing myofibrils (Figs 3, 4 and 6–14), large glycogen deposits (Figs 4 and 9), lipid droplets (Figs 3 and 4), mitochondria (Figs 3, 4 and 8), rough endoplasmic reticulum (Fig. 10), sarcoplasmic reticulum (Figs 7 and 11–13) and caveolae (Fig. 13). Noteworthy, intercellular junctions (Figs 6 and 14) were formed by desmosomes and fascia adherens.

Myofibrils

All cells in the EB had myofibrils in the cytoplasm, the main feature defining cardiomyocytic differentiation of HFKT-iPSC and

Table 1 Comparative analysis of structural and morphometric aspects of hESC-CM and HFKT-iPSC-CM

Parameter	hESC-CM	HFKT-iPSC-CM	*P*-value
Cell area (μm^2)	42.54 $\pm$ 16.9	58.65 $\pm$ 20.15	$P < 0.01$
Nucleus area (μm^2)	16.53 $\pm$ 6.72	19.71 $\pm$ 7.22	N.S.
Cytoplasm area (μm^2)	26.01 $\pm$ 13.88	38.93 $\pm$ 18.99	$P < 0.01$
Cell length (μm)	9.68 $\pm$ 3.06	11.93 $\pm$ 3.99	$P < 0.05$
Cell width (μm)	6.21 $\pm$ 1.85	6.89 $\pm$ 1.79	N.S.
Ratio NC/CY	0.88 $\pm$ 0.40	0.62 $\pm$ 0.33	N.S.

Note: In each group, 28 cardiomyocytes were analysed. The analysis included three EBs from each group. NC/CY: nucleus/cytoplasm.

hESC (Figs 6 and 7). The myofibrils showed variable degrees of organization as sarcomeres (Fig. 6). Myofilaments were present in the cardiomyocytes, and usually were organized in myofibrils with a sarcomeric pattern in both HFKT-iPSC-CM (Fig. 7A) and hESC-CM (Fig. 7B). The myofibrils had a winding flow into the cells with straight segments formed by up to eight sarcomeres in HFKT-iPSC-CM, and up to seven sarcomeres in hESC-CM (counted in 28 cells for each type of EB). Sarcomeres mean length was 1.50 $\pm$ 0.15 μm in HFKT-iPSC-CM and 1.53 $\pm$ 0.16 μm in hESC-CM. Z-bands (about 50-nm thick) had variable span from 0.1 to 2.25 μm (mean: 0.99 $\pm$ 0.56 μm for HFKT-iPSC-CM and 1.03 $\pm$ 0.62 μm for hESC-CM). No other bands were visible in the sarcomeres construct neither in HFKT-iPSC-CM nor in hESC-CM. The myofibrils were inserted into the developing intercalated disc at the level of fascia adherens (Fig. 14).

Mitochondria

Electron microscopy showed that mitochondria have similar aspect and distribution in HFKT-iPSC-CM (Fig. 8A) and hESC-CM (Fig. 8B). Long (up to 6 μm; Fig. 9A) and slender (0.2–0.5 μm) mitochondria were clustered in small groups next to the nucleus (Fig. 3) or in the periphery (Fig. 4) of cardiomyocytes. The nano-contacts linking mitochondria and sarcoplasmic reticulum cisternae were rare (Fig. 9B), although these two organelles were closely associated (Fig. 8).

Sarcoplasmic/endoplasmic reticulum

HFKT-iPSC-CM (Fig. 10A) and hESC-CM (Fig. 10B) equally presented conspicuous rough endoplasmic reticulum and poorly developed sarcoplasmic reticulum (Figs 11 and 12). Few sarcoplasmic reticulum cisterns were peripherally coupled with the plasma membrane by small dense structures ('feet'). Such 'Ca^{2+}
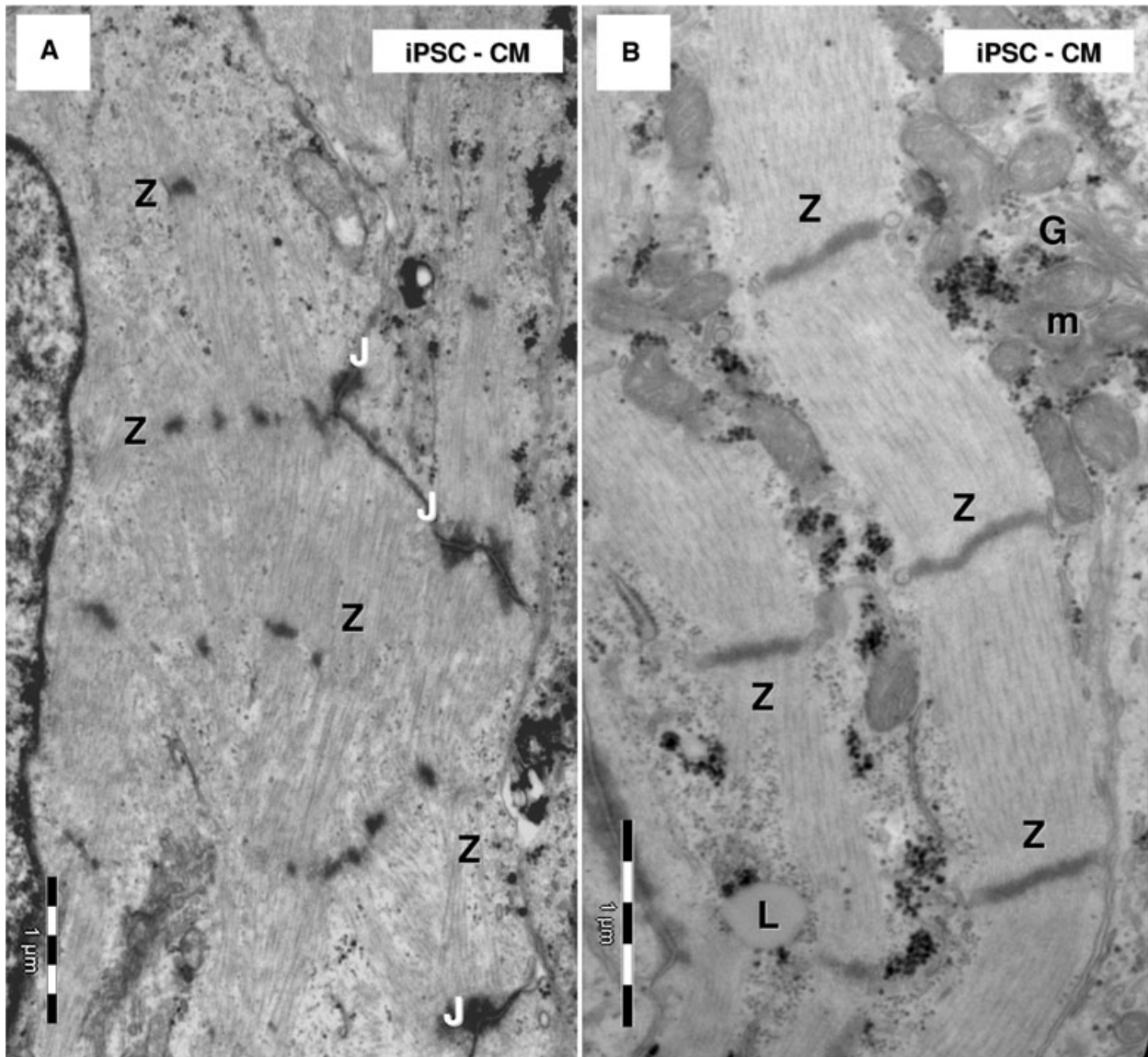
Fig. 6 Electron microscopy of HFK-iPSC-CM. Note highly organized myofilaments which form myofibrils (**A**) or myofibrils lacking alignment (**B**) in HFK-iPSC-CM. (**A**) Z-like dense structures connect bundles of myofilaments. (**B**) Z-bands clearly show sarcomere limits along myofibrils. J: junctions; L: lipid droplet; m: mitochondria; G: Golgi system.

release units' were present in the differentiated cardiomyocytes (Figs 11 and 12), although they were infrequent.

Caveolae

The plasma membrane of differentiated cardiomyocytes showed caveolae (Fig. 13) and coated pits. On oblique sections through the plasmalemma it was obvious that sarcoplasmic reticulum cisternae surround caveolae (Fig. 13). The basal lamina (Fig. 13) was visible on the plasmalemma of the cardiomyocytes.

Other organelles

Other organelles equally visible in HFKT-iPSC-CM and hESC-CM were well-developed Golgi system (Figs 6B and 8B), lysosomes, centrioles, ribosomes (Fig. 7) and inconspicuous dense granules. Semi-quantitative assessment of ultrastructural features showed that the organelles were similarly developed in HFKT-iPSC-CM and hESC-CM (Fig. 15A) but differentiation was not uniform into the EBs (Fig. 15B). The HFKT-iPSC-CM and hESC-CM in the periphery of the EBs showed more mature phenotype than those in the centre.
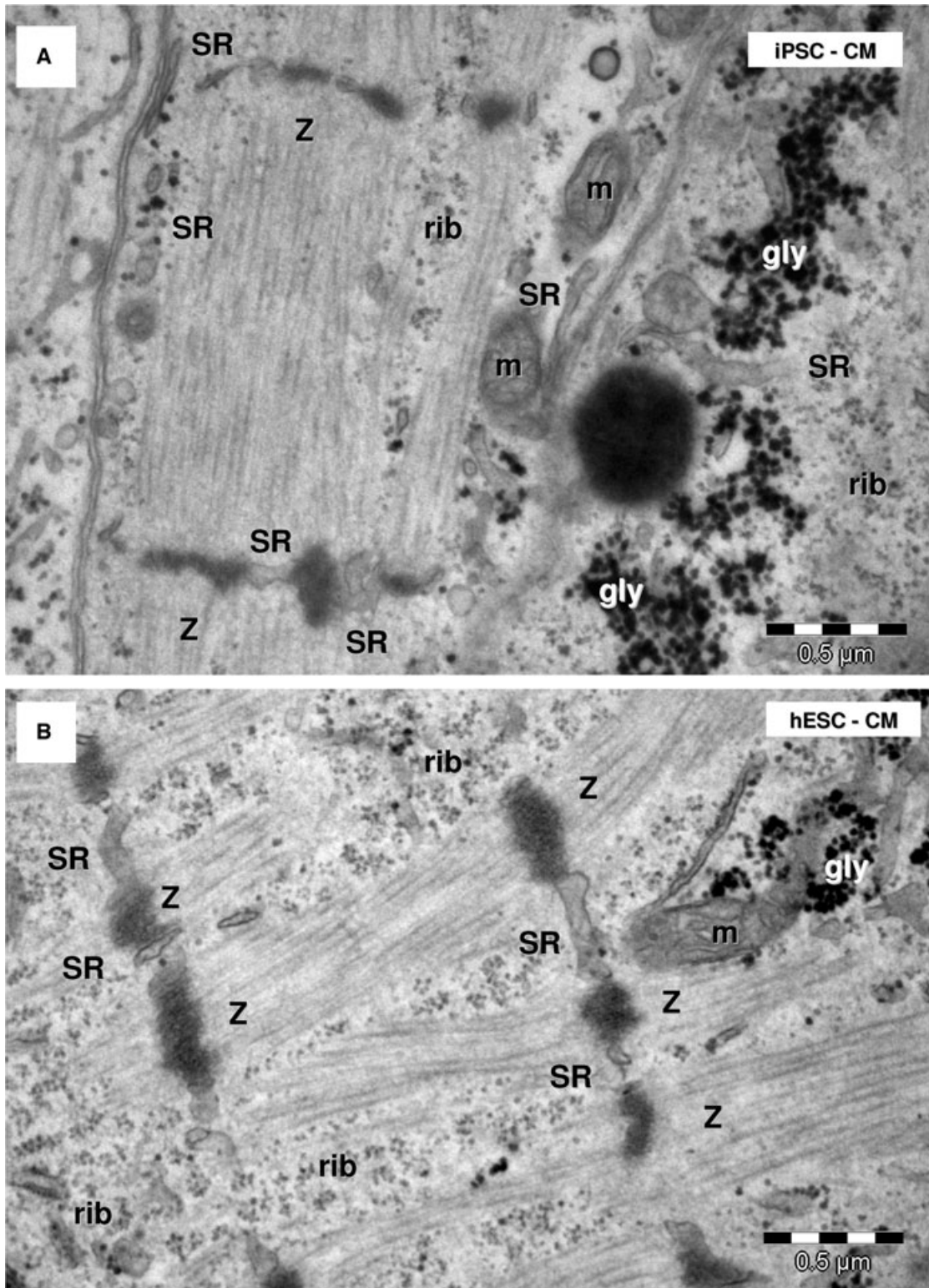
Fig. 7 Electron microscopy shows myofibrils with sarcomeric pattern in HFK-iPSC-CM (**A**) and hESC-CM (**B**). Sarcoplasmic reticulum cisternae (SR) are visible between Z-bands. m: mitochondria; rib: free ribosomes; gly: glycogen granules.
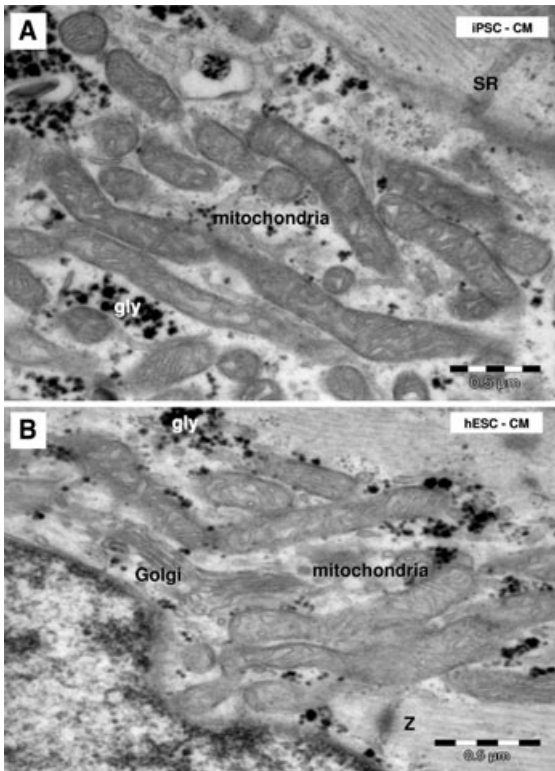
Fig. 8 Electron microscopy shows clusters of long and slender mitochondria in HFK-iPSC-CM (**A**) and hESC-CM (**B**). SR: sarcoplasmic reticulum; gly: glycogen granules; Z: Z band.
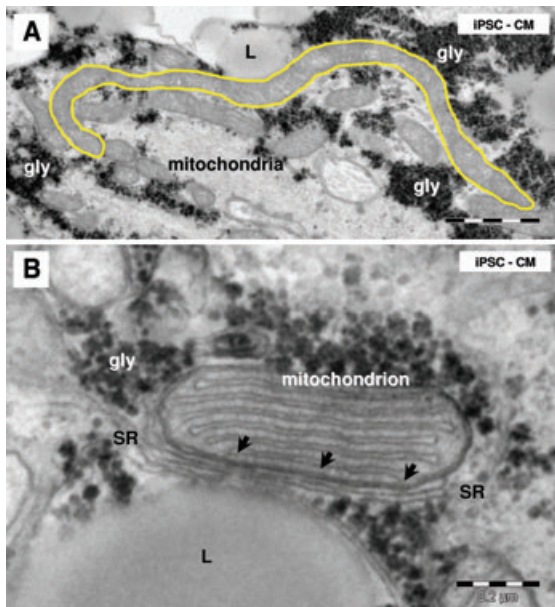

Fig. 10 Electron microscopy shows conspicuous rough endoplasmic reticulum (rER) in HFK-iPSC-CM (**A**) and hESC-CM (**B**). m: mitochondria; rib: ribosomes; L: lipid droplet; gly: glycogen.

Fig. 9 Electron microscopy of iPSC-CM mitochondria. (**A**) Note a long mitochondrion (yellow outlined; 6 μm). (**B**) Small dense structures (arrows) connect sarcoplasmic reticulum (SR) with a mitochondrion. L: lipid droplets; gly: glycogen.
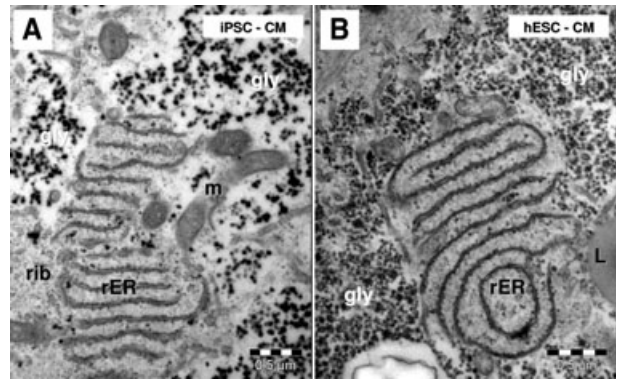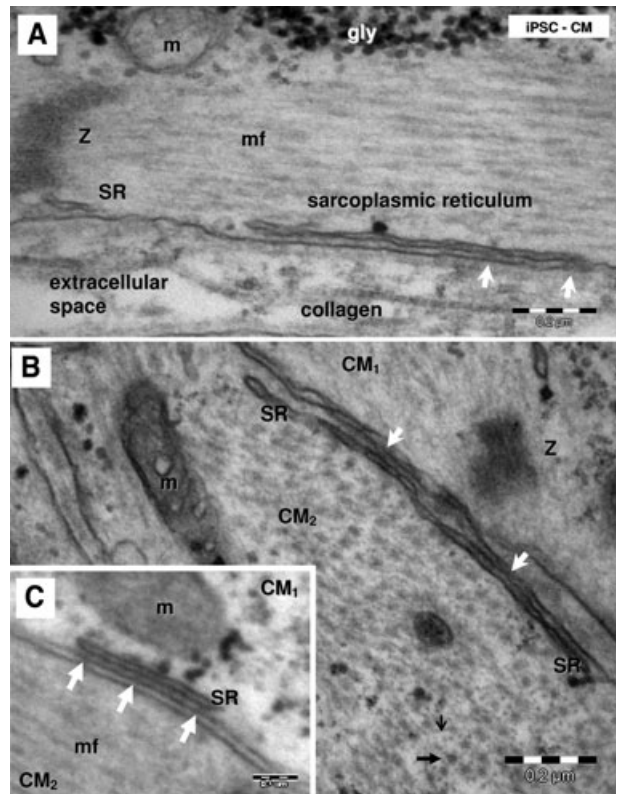

Fig. 11 Electron micrographs (**A–C**) show peripheral couplings or 'Ca^{2+} release units' in HFK-iPSC-CM visible as small dense structures (white arrows) between peripheral sarcoplasmic reticulum (SR) and plasmalemma. Longitudinally (**A**) and transversally (**B**) sectioned myofilaments. Thin (small black arrow) and thick (thick black arrow) myofilaments are visible in the transverse section (**B**). Z: Z bands; gly: glycogen; mf: myofilaments; m: mitochondria; CM1 and CM2: indicates that these are different adjacent cardiomyocytes.
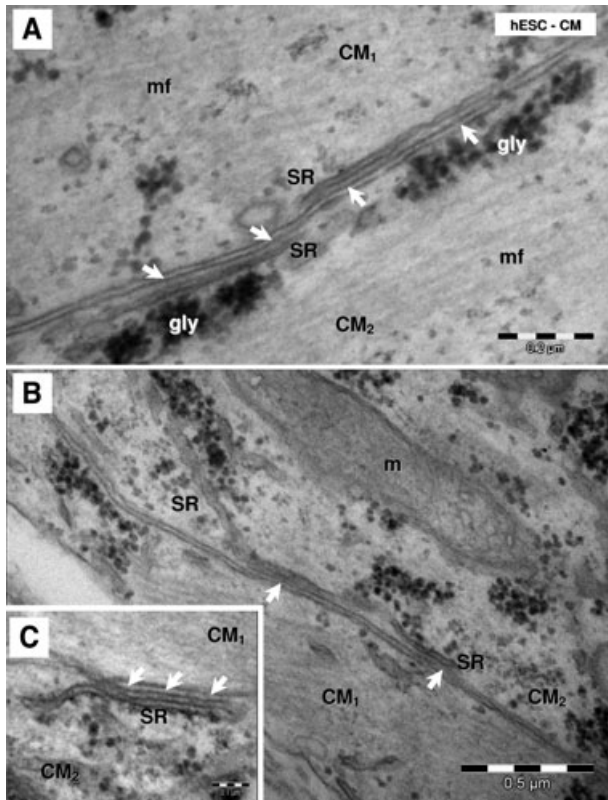
Fig. 12 Electron micrographs (**A–C**) show 'Ca^{2+} release units' (white arrows) connecting peripheral sarcoplasmic reticulum (SR) and plasmalemma in hESC-CM. gly: glycogen; mf: myofibrils; m: mitochondria; CM1 and CM2: indicates that these are different adjacent cardiomyocytes.

Fig. 13 Electron microscopy shows caveolae on plasmalemma of HFK-iPSC-CM (**A**) and hESC-CM (**B**). Tangent sections of cardiomyocytes plasmalemma show the caveolae surrounded by the peripheral sarcoplasmic reticulum (SR). m: mitochondria; rER: rough endoplasmic reticulum; L: lipid droplets; ECS: extracellular space.

Intercellular junctions

Differentiated cardiomyocytes were connected by desmosomes and fascia adherens often forming together junctional complexes (Fig. 14), but no canonical intercalated disks with typical step ladder pattern were found. We often found adherens junctions connecting the cellular processes of cardiomyocytes that protruded into neighbouring cardiomyocytes. Finally, gap junctions were not clearly identified by electron microscopy either in HFKT-iPSC-CM or in hESC-CM.

Discussion

The aim of this study was to compare the ultrastructural features of cardiomyocytes differentiated from iPSC (generated from human hair follicle keratinocytes), with hESC-CM. The major finding of our study was the demonstration of an *efficient differentiation* of HFKT-iPSC i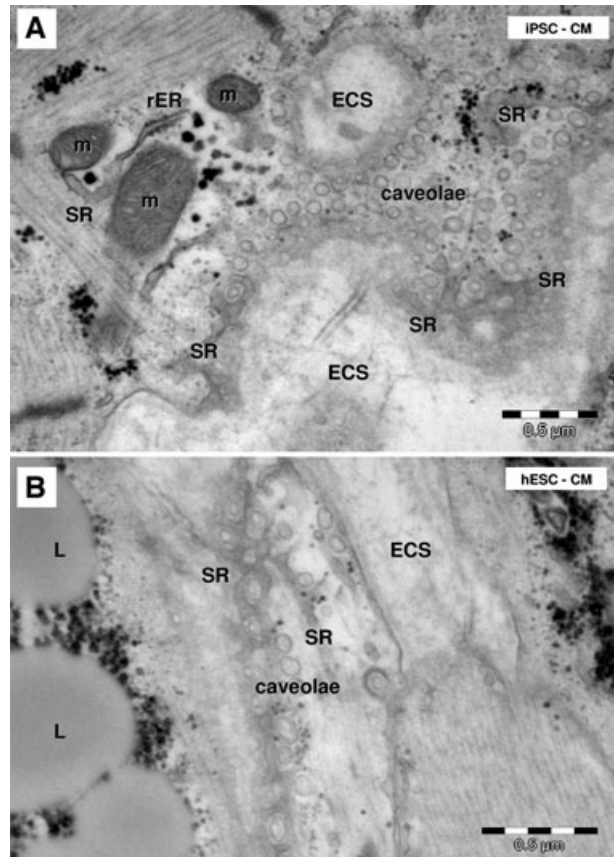nto cardiomyocytes. These cells have parallel arrays of myofibrils organized into sarcomeres separated by Z bands, junctional sarcoplasmic reticulum and caveolae. HFKT-iPSC-CM are connected by junctional complexes formed by desmosomes and fascia adherens. Anyway, this study shows that HFKT-iPSC-CM have an ultrastructure similar to the ultrastructural aspect of hESC-CM, which has already been described [11,12].

In support of our previous report, this study also shows that HFKT are easily obtainable, highly reprogrammable human cell source for iPSC, and their use for cardiac differentiation is efficient and promising [4]. Structurally, HFKT-iPSC-CM have an immature cardiac ultrastructural phenotype at 31-days of culture, expressed by numerous lipid droplets, high glycogen contents, abundant rough endoplasmic reticulum and variable degrees of myofibrillar organization. We could observe sparse and relatively unorganized myofibrillar bundles in the central cardiomyocytes compared with peripheral cardiomyocytes. The same differences in maturation were observed in EBs derived from hESC. Interestingly, Rajala *et al.* [13] recently reported that cardiomyocytes induction from pluripotent stem cells resulted in mixtures of ventricular-like,
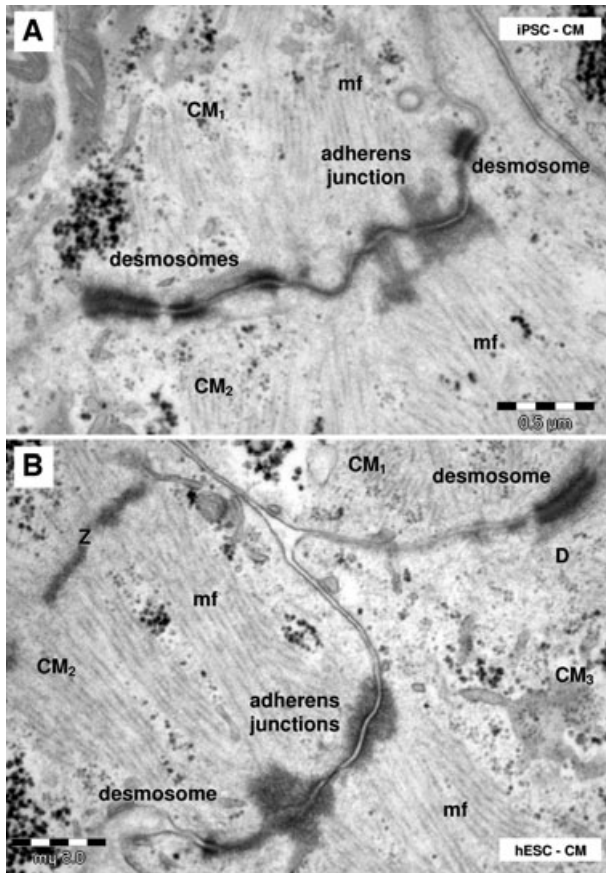
Fig. 14 Electron microscopy shows desmosomes and adheres junctions connecting HFK-iPSC-CM (**A**) and hESC-CM (**B**). CM₁–CM₃: different cardiomyocytes; Z: Z-bands; mf: myofilaments.

Fig. 15 (**A**) Comparative representation of semi-quantitative assessment of the ultrastructural features of HFKT-iPSC-CM and hESC-CM. (**B**) Comparative representation of semi-quantitative assessment of the ultrastructural features of peripheral (CM_p) and central (CM_c) located cardiomyocytes into the embryoid bodies. rER: rough endoplasmic reticulum; SR: sarcoplasmic reticulum.

atrial-like and pacemaker-like cells defined by intracellular electro-physiological measurements of action potentials. The presence of cardiomyocytes at different developmental stages in the same EB, may underlie the mixed physiological results. In this study we did not find evidence for different sub-types of cardiomyocytes, but we found that HFKT-iPSC-CM located in the middle of the EB have a more immature phenotype than peripheral cardiomyocytes. These findings raise questions regarding the conditions required for: (1) developing a homogenous phenotype of cardiomyocytes from iPSC or hESC and (2) generating evenly mature iPSC-derived cardiomyocytes *in vitro.*

Intercellular communications

The derived cardiomyocytes were connected through complex adhering structures or 'primitive' intercalated disks formed by desmosomes and fascia adherens, but no gap junctions were observed in 31-day-old cultured HFKT-iPSC-CM or hESC-CM. The presence of gap junction seems not essential for intercalated disks
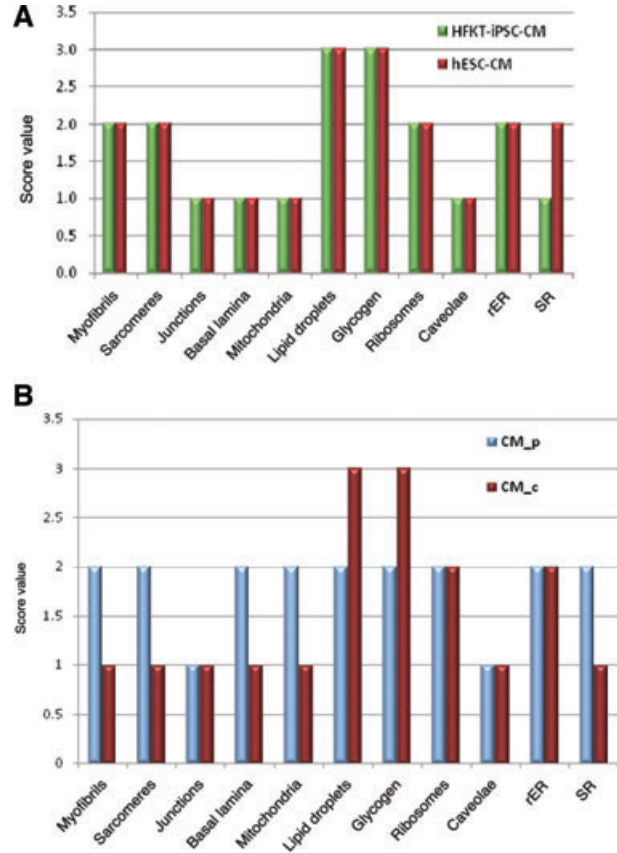
formation [14], but adhering type of junction is the prerequisite for subsequent gap junction formation within the intercalated disk [15]. The progressive accumulation of gap junctions in intercalated disks is noted after birth, and a pattern of association between gap junctions and cell adhesion junctions is likely to be an important factor in maturation of electromechanical function of the heart [16].

The sarcoplasmic reticulum, caveolae and mitochondria

The ultrastructural analysis in HFKT-iPSC-CM and hESC-CM revealed the presence of 'Ca^{2+} release units' constituted as specialized junctional domains of the peripheral sarcoplasmic reticulum, which commonly express Ca^{2+} release channels (ryanodine receptors). Nonetheless, the actual presence of these structures does not indicate whether or not they are functional. T tubules

were not observed, but the biogenesis of T tubules and the formation of dyads is an event that occurs relatively late in mammalian cardiomyocytes development [17–19]. Indeed, it was reported that in mammals cardiomyocytes contain sarcoplasmic reticulum and peripheral-couplings very early during embryogenesis with a putative role in excitation–contraction coupling [20]. Our analysis further demonstrated that cardiomyocytes from both groups contained caveolae, which were isolated or clustered and surrounded by sarcoplasmic reticulum cisternae.

Caveolae formation seems to be a necessary step in the invagination process of T tubules, and caveolin plays an essential role in this process by allowing membrane curving [21]. Moreover, Xiang *et al.* [22] reported that caveolae host adrenergic receptors, and that this localization is essential for physiologic signalling. Another important finding in HFKT-iPSC-CM and hESC-CM are small dense structures, which connect the sarcoplasmic reticulum with mitochondria. These connections play an important role not only for calcium signalling in smooth muscle cell [10, 23, 24] and striated muscle [25], but also in the heart [25, 26].

In conclusion, this study shows that HFKT-iPSC-CM and hESC-CM have similar ultrastructure and compartmentalized phenotypes: embryonal cardiomyocytes in the centre of the EB and foetal cardiomyocytes in the periphery. Hence, it remains to be investigated how to generate a homogenous cardiomyocytes population *in vitro*. One feasible option is to co-culture the iPSC-CM with cardio-inductive cells or, particularly, with newly described telocytes [27–31] which seem to have an important role in cardiac development [32] and cardiac regeneration [29, 33].

Perspectives, HFKT-iPSC differentiate into cardiomyocytes with similar ultrastructure to hESC-CM, and therefore iPSC-CM constitute a viable option for an autologous cell source for cardiac regenerative therapy, as well as for investigating the mechanisms underlying inherited cardiac diseases such as Long QT syndrome [34].

Acknowledgements

Conflict of interest

The authors declare no conflict of interest.

References

1. **Takahashi K, Yamanaka S.** Induction of pluripotent stem cells from mouse embryonic and adult fibroblast cultures by defined factors. *Cell.* 2006; 126: 663–76.
2. **Takahashi K, Tanabe K, Ohnuki M, *et al.*** Induction of pluripotent stem cells from adult human fibroblasts by defined factors. *Cell.* 2007; 131: 861–72.
3. **Germanguz I, Sedan O, Zeevi-Levin N, *et al.*** Molecular characterization and functional properties of cardiomyocytes derived from human inducible pluripotent stem cells. *J Cell Mol Med.* 2011; 15: 38–51.
4. **Novak A, Shtrichman R, Germanguz I, *et al.*** Enhanced reprogramming and cardiac differentiation of human keratinocytes derived from plucked hair follicles, using a single excisable lentivirus. *Cell Reprogramm.* 2010; 12: 665–78.
5. **Fujiwara M, Yan P, Otsuji TG, *et al.*** Induction and enhancement of cardiac cell differentiation from mouse and human induced pluripotent stem cells with cyclosporine-A. *PLoS One.* 2011; 6:e16734. doi:10.1371/journal.pone.0016734
6. **Dolnikov K, Shilkrut M, Zeevi-Levin N, *et al.*** Functional properties of human embryonic stem cell-derived cardiomyocytes: intracellular Ca^{2+} handling and the role of sarcoplasmic reticulum in the contraction. *Stem Cells.* 2006; 24: 236–45.
7. **Meiry G, Reisner Y, Feld Y, *et al.*** Evolution of action potential propagation and repolarization in cultured neonatal rat ventricular myocytes. *J Cardiovasc Electrophysiol.* 2001; 12: 1269–77.
8. **Reisner Y, Meiry G, Zeevi-Levin N, *et al.*** Impulse conduction and gap junctional remodelling by endothelin-1 in cultured neonatal rat ventricular myocytes. *J Cell Mol Med.* 2009; 13: 562–73.
9. **Mandache E, Popescu LM, Gherghiceanu M.** Myocardial interstitial Cajal-like cells (ICLC) and their nanostructural relationships with intercalated discs: shed vesicles as intermediates. *J Cell Mol Med.* 2007; 11: 1175–84.
10. **Popescu LM, Gherghiceanu M, Mandache E, *et al.*** Caveolae in smooth muscles: nanocontacts. *J Cell Mol Med.* 2006; 10: 960–90.
11. **Kehat I, Kenyagin-Karsenti D, Snir M, *et al.*** Human embryonic stem cells can differentiate into myocytes with structural and functional properties of cardiomyocytes. *J Clin Invest.* 2001; 108: 407–14.
12. **Snir M, Kehat I, Gepstein A, *et al.*** Assessment of the ultrastructural and proliferative properties of human embryonic stem cell-derived cardiomyocytes. *Am J Physiol Heart Circ Physiol.* 2003; 285: H2355–63.
13. **Rajala K, Pekkanen-Mattila M, Aalto-Setälä K.** Cardiac differentiation of pluripotent stem cells. *Stem Cells Int.* 2011; 2011: 383709. doi: 10.4061/2011/383709
14. **Gutstein DE, Liu FY, Meyers MB, *et al.*** The organization of adherens junctions and desmosomes at the cardiac intercalated disc is independent of gap junctions. *J Cell Sci.* 2003; 116: 875–85.
15. **Kostin S, Hein S, Bauer EP, *et al.*** Spatiotemporal development and distribution of intercellular junctions in adult rat

cardiomyocytes in culture. *Circ Res.* 1999; 85: 154–67.

16. **Angst BD, Khan LU, Severs NJ,** *et al.* Dissociated spatial patterning of gap junctions and cell adhesion junctions during postnatal differentiation of ventricular myocardium. *Circ Res.* 1997; 80: 88–94.

17. **Popescu LM**. Conceptual model of the excitation-contraction coupling in smooth muscle; the possible role of the surface microvesicles. *Studia Biophys (Berlin).* 1974; 44: 141–53.

18. **Di Maio A, Karko K, Snopko RM,** *et al.* T-tubule formation in cardiac myocytes: two possible mechanisms? *J Muscle Res Cell Motil.* 2007; 28: 231–41.

19. **Ziman AP, Gómez-Viquez NL, Bloch RJ,** *et al.* Excitation-contraction coupling changes during postnatal cardiac development. *J Mol Cell Cardiol.* 2010; 48: 379–86.

20. **Franzini-Armstrong C, Protasi F, Tijskens P.** The assembly of calcium release units in cardiac muscle. *Ann N Y Acad Sci.* 2005; 1047: 76–85.

21. **Parton RG, Way M, Zorzi N,** *et al.* Caveolin-3 associates with developing T-tubules during muscle differentiation. *J Cell Biol.* 1997; 136: 137–54.

22. **Xiang Y, Rybin VO, Steinberg SF,** *et al.* Caveolar localization dictates physiologic signaling of beta 2-adrenoceptors in neonatal cardiac myocytes. *J Biol Chem.* 2002; 277: 34280–6.

23. **Gherghiceanu M, Popescu LM.** Caveolar nanospaces in smooth muscle cells. *J Cell Mol Med.* 2006; 10: 519–28.

24. **Gherghiceanu M, Popescu LM.** Electron microscope tomography: further demonstration of nanocontacts between caveolae and smooth muscle sarcoplasmic reticulum. *J Cell Mol Med.* 2007; 11: 1416–8.

25. **Franzini-Armstrong C.** ER-mitochondria communication: how privileged? *Physiology (Bethesda)* 2007; 22: 261–8.

26. **Hayashi T, Martone ME, Yu Z,** *et al.* Three-dimensional electron microscopy reveals new details of membrane systems for Ca^{2+} signaling in the heart. *J Cell Sci.* 2009; 122: 1005–13.

27. **Kostin S, Popescu LM.** A distinct type of cell in myocardium: interstitial Cajal-like cells (ICLCs). *J Cell Mol Med.* 2009; 13: 295–308.

28. **Popescu LM, Faussone-Pellegrini MS**. TELOCYTES-a case of serendipity: the winding way from Interstitial Cells of Cajal (ICC), *via* Interstitial Cajal-Like Cells (ICLC) to TELOCYTES. *J Cell Mol Med.* 2010; 14: 729–40.

29. **Popescu LM, Gherghiceanu M, Kostin S,** *et al.* Telocytes and heart renewing. In: Wang P, Kuo CH, Takeda N, Singal PK, editors. Adaptation biology and medicine, vol. 6. Cell adaptations and challenges. Narosa: New Delhi; 2011. pp. 17–39.

30. **Popescu LM.** The tandem: telocytes-stem cells. *Intl J Biol Biomed Eng.* 2011; 5: 83–92.

31. **Faussone-Pellegrini MS, Popescu LM.** Telocytes. *BioMolecular Concepts.* 2011; doi: 10.1515/BMC.2011.039.

32. **Bani D, Formigli L, Gherghiceanu M,** *et al.* Telocytes as supporting cells for myocardial tissue organization in developing and adult heart. *J Cell Mol Med.* 2010; 14: 2531–8.

33. **Gherghiceanu M, Popescu LM.** Cardiomyocyte precursors and telocytes in epicardial stem cell niche: electron microscope images. *J Cell Mol Med.* 2010; 14: 871–7.

34. **Moretti A, Bellin M, Welling A,** *et al.* Patient-specific induced pluripotent stem-cell models for long-QT syndrome. *N Engl J Med.* 2010; 363: 1397–409.